Physics Letters B 307 (1993) 394–398
North-Holland

PHYSICS LETTERS B

Evidence for $\eta\eta$ resonances in antiproton–proton annihilations at $2950 < \sqrt{s} < 3620$ MeV

T.A. Armstrong[f], D. Bettoni[b], V. Bharadwaj[a], C. Biino[g], G. Borreani[b], D. Broemmelsiek[d], A. Buzzo[c], R. Calabrese[b], A. Ceccucci[g], R. Cester[g], M. Church[a], P. Dalpiaz[b], P.F. Dalpiaz[b], R. Dibenedetto[g], D. Dimitroyannis[e], M.G. Fabbri[b], J. Fast[d], A. Gianoli[b], C.M. Ginsburg[e], K. Gollwitzer[d], A. Hahn[a], M. Hasan[f], S. Hsueh[a], R. Lewis[f], E. Luppi[b], M. Macrí[c], A.M. Majewska[f], M. Mandelkern[d], F. Marchetto[g], M. Marinelli[c], J. Marques[d], W. Marsh[a], M. Martini[b], M. Masuzawa[e], E. Menichetti[g], A. Migliori[g], R. Mussa[g], M. Pallavicini[c], S. Palestini[g], N. Pastrone[g], C. Patrignani[c], J. Peoples Jr.[a], L. Pesando[g], F. Petrucci[b], M.G. Pia[c], S. Pordes[a], P. Rapidis[a], R. Ray[e,a], J. Reid[f], G. Rinaudo[g], B. Roccuzzo[g], J. Rosen[e], A. Santroni[c], M. Sarmiento[e], M. Savrie[b], A. Scalisi[c], J. Schultz[d], K.K. Seth[e], A. Smith[d], G.A. Smith[f], M. Sozzi[g], S. Trokenheim[e], M.F. Weber[d], S. Werkema[a], Y. Zhang[f], J. Zhao[e] and G. Zioulas[d]

[a] *Fermi National Accelerator Laboratory, Batavia, IL 60510, USA*
[b] *INFN and University of Ferrara, 44100 Ferrara, Italy*
[c] *INFN and University of Genoa, 16146 Genoa, Italy*
[d] *University of California at Irvine, Irvine, CA 92717, USA*
[e] *Northwestern University, Evanston, IL 60208, USA*
[f] *Pennsylvania State University, University Park, PA 16802, USA*
[g] *INFN and University of Turin, 10125 Turin, Italy*

Received 8 April 1993
Editor: L. Montanet

We present the first high-statistics study of the $\eta\eta$ system over the mass range 1000–3000 MeV/c^2. The experiment was performed at the Fermilab Antiproton Accumulator, and the data sample consists of six-photon final states produced in antiproton–proton annihilations at $\sqrt{s}$ in the range 2950–3620 MeV. We find evidence for three states with masses 1488 ± 10 MeV/c^2, 1748 ± 10 MeV/c^2 and 2104 ± 20 MeV/c^2 respectively.

We have studied the spectrum of light quark mesons using data obtained in an experiment to investigate the resonant formation of charmonium in proton–antiproton annihilations. The features of the experimental setup, which includes a small interaction region as defined by a circulating antiproton beam and a hydrogen gas-jet target and a large, fine grained electromagnetic calorimeter, combine to provide the possibility of measuring photon energies and directions with good resolution over a large acceptance. The data reported in this paper were taken in conjunction with data-taking at the $\eta_c(2980)$, $J/\psi(3097)$, ${}^1P_1(3526)$ and unconfirmed $\eta_c'(3590)$ charmonium resonances.

The E-760 detector has been described in previous publications [1]. We review here only the features relevant to the detection of neutral final states. The detector is located in the AP50 straight section of the Fermilab Antiproton Accumulator Ring and is a nonmagnetic spectrometer with cylindrical symmetry and full azimuthal coverage. It consists of a central lead glass barrel calorimeter (CCAL) with polar angle acceptance ranging from 12° to 70°, and a forward scintillator/lead sandwich calorimeter (FCAL) with coverage down to 2°. A silicon detector located at $\theta = 86.5°$ measures the recoil proton spectrum and serves as a luminosity monitor.

CCAL is comprised of 1280 lead glass blocks pointing to the interaction source, arranged in 20 "rings" and 64 "wedges". The energy resolution of CCAL is $\sigma(E)/E = 6\%/\sqrt{E\ (\mathrm{GeV})} + 1.4\%$. The combina-

Elsevier Science Publishers B.V.

tion of a small source size and good calorimeter granularity yields a precision in the measured direction of photons of $\sigma(\theta) = 5.7$ mrad and $\sigma(\phi) = 12.3$ mrad.

To achieve acceptable rates for charmonium events, luminosities of up to 8×10^{30} $\mathrm{cm^{-2}s^{-1}}$ are required with a circulating beam of 4×10^{11} antiprotons at a frequency of about 0.63 MHz, and an internal hydrogen gas-jet target density of about 5×10^{13} atoms/cm^3. The small size of the interaction region is defined transversely by the dimension of the beam (about 3.5 mm for 95% containment) and longitudinally by the thickness of the gas jet (about 6 mm).

To form the trigger, analog sums of signals from CCAL were combined into an overall energy sum, which was discriminated at a threshold corresponding to approximately 85% of the interaction energy. Veto signals from two scintillator hodoscopes (H1 and Veto Counter) were used to define neutral events. Because of excessive rates in the forward direction, which would lead to undesired deadtime in the accumulation of charmonium data, a veto from the forward calorimeter (FCAL) was normally added to the trigger. Triggered events were then processed using the Fermilab ACP system, where the total energy deposited was calculated, and only events with more than 90% of the available energy were recorded.

Offline analysis identified each 3 × 3 grid of lead glass cells, with a local maximum energy at the center block, to be a single photon. Details of the reconstruction algorithm (e.g. separation of overlapping clusters, rejection of pile-up) are discussed elsewhere [2]. Events were saved for further analysis if there were six identified photons in CCAL and none in FCAL. Each event was kinematically fitted to a six-photon hypothesis with the constraints of total four-momentum conservation. Two-photon invariant masses were then calculated for all 15 pairs (fig. 1a), and each pair with an invariant mass in the range 70–200 MeV/c^2 (470–630 MeV/c^2) was identified as coming from a π^0 (η) decay into two photons. The η signal, as well as $\omega(783)$ and $\eta'(958)$ signals, are enhanced by rejecting all two-photon pairs in the π^0 window (inset, fig. 1a). Events were then kinematically fitted to

$$\bar{p} + p \to \pi^0 + \pi^0 + \pi^0, \qquad (1)$$

$$\bar{p} + p \to \pi^0 + \pi^0 + \eta, \qquad (2)$$

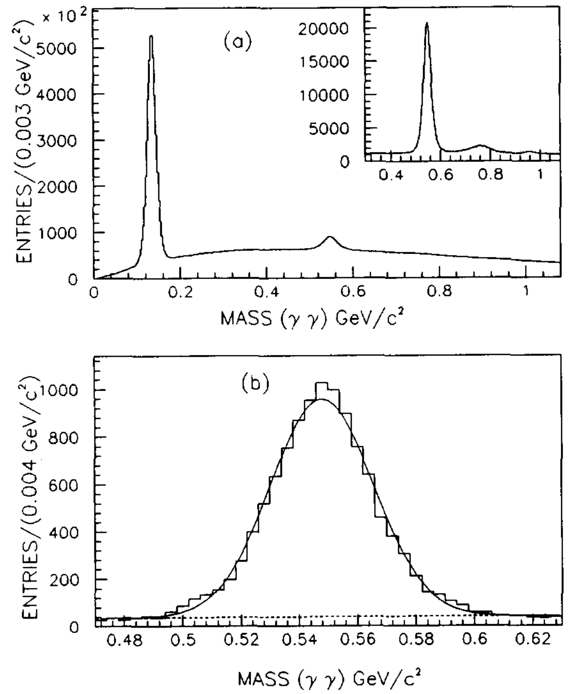

Fig. 1. (a) Two-gamma invariant mass distributions from six-gamma events. The inset shows gamma's not associated with π^0 decay. See text for details. (b) Two-gamma invariant mass distribution for reaction (4) at 3.5 GeV CM energy. The solid (dotted) curves are fits to gaussian (linear) forms for the η signal (background). See text for details.

$$\bar{p} + p \to \pi^0 + \eta + \eta, \qquad (3)$$

and

$$\bar{p} + p \to \eta + \eta + \eta. \qquad (4)$$

The two hypotheses with the highest probabilities were saved, and if either of the photons from an η candidate combines with any other photon to form a mass in the range 110–160 MeV/c^2, the event was flagged. In the final data-sample, only events with a fit probability greater than 10%, above which the distribution was flat, were retained. In addition, events fitted to reactions (2)–(4) were rejected if the above flag was set, and for reactions (3) and (4) we required also that the probability of the second best hypothesis should be less than 0.01%. We have simulated reactions (3) and (4) using pure phase space and isotropic production angular distri-

Table 1
Integrated luminosities and numbers of fits to each hypothesis.

$\sqrt{s}$ (GeV)	Integrated luminosities (pb^{-1})	$3\pi^0$	$2\pi^0 + \eta$	$\pi^0 + 2\eta$	3η
3.0	3.07	2.19×10^6	7.15×10^5	5.19×10^4	3.50×10^3
3.5	18.35	1.46×10^6	4.68×10^5	7.30×10^4	6.43×10^3

butions to estimate the percentage of events rejected by these cuts, which is approximately 30%. The rejected events have an $\eta\eta$ mass distribution which is smoothly varying from 1100–2800 MeV/c^2. Table 1 summarizes the data-sample, with the numbers of fits to each reaction, where we have grouped the data in two energy samples for convenience. Reactions (1), (2) are the subject of a separate paper [3].

As an illustration of the levels of background present, we show in fig. 1b the data from the 3η reaction at 3.5 GeV, where we plot two-photon mass combinations in the η mass window after the six-photon kinematic fit. Fitting to a gaussian together with a first-order polynomial to describe the background, we find a mass, RMS width and integrated background (dotted curve) equal to 547.9 ± 0.2 MeV/c^2, 17.7 ± 0.2 MeV/c^2 and 13.3% respectively. For reaction (3) the integrated background under the π^0 peak is 2.3%, and for the η it is 12.3%. These represent upper limits, as kinematic fitting to reactions (3) and (4) has not yet been attempted.

The Dalitz plots for reaction (3) shown in figs. 2a and 2b are complex, with many crossing bands present. In addition to $\eta\eta$ states, we also have to consider the spectrum of $\eta\pi$ states. Bands corresponding to the $a_0(980)$ and $a_2(1320)$ are present, and in both plots at least three states decaying to $\eta\eta$, at 1500 MeV/c^2, 1750 MeV/c^2 and 2100 MeV/c^2 are strongly suggested. These are also visible in the mass projections shown in figs. 3a and 3b.

The CM production angle acceptance for a state decaying to $\eta\eta$ in this experiment is limited to approximately $|\cos(\theta^*_X)| < 0.5$. We have calculated the dependence of the acceptance on the mass of the $\eta\eta$ pair, for various production and decay distributions. We find the acceptance to be typically 15% overall, and to be a smoothly varying function over the $\eta\eta$ mass range in question.

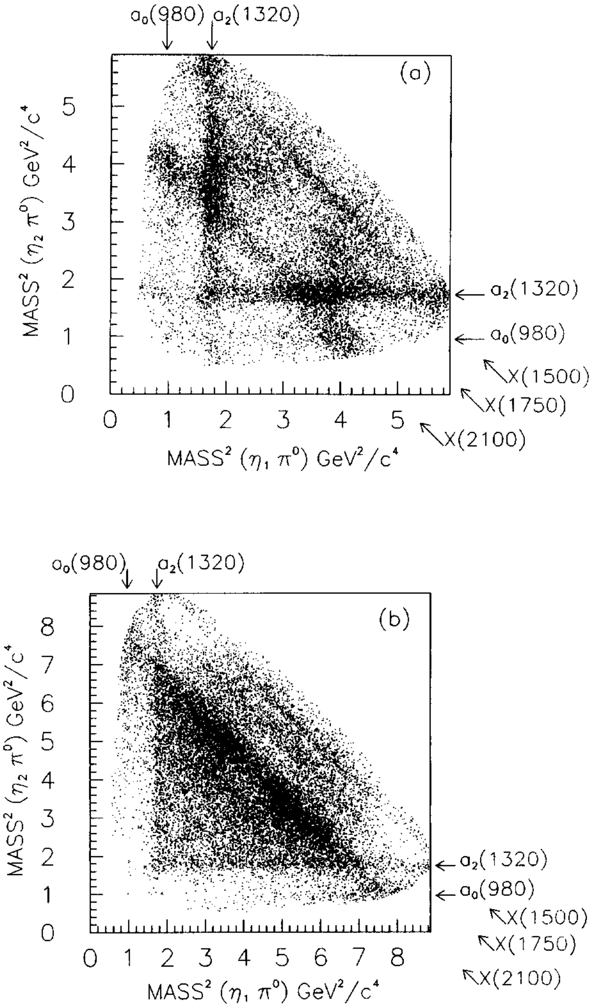

Fig. 2. Dalitz plots for reaction (3) at (a) 2980 and (b) 3526 MeV CM energy.

Fitting the $\eta\eta$ mass projections of figs. 3a and 3b to three Breit–Wigner structures plus a polynomial background over the full mass range (fig. 3a) and up to 2250 MeV/c^2 (fig. 3b) gives the following average values for the masses and widths of the three features:

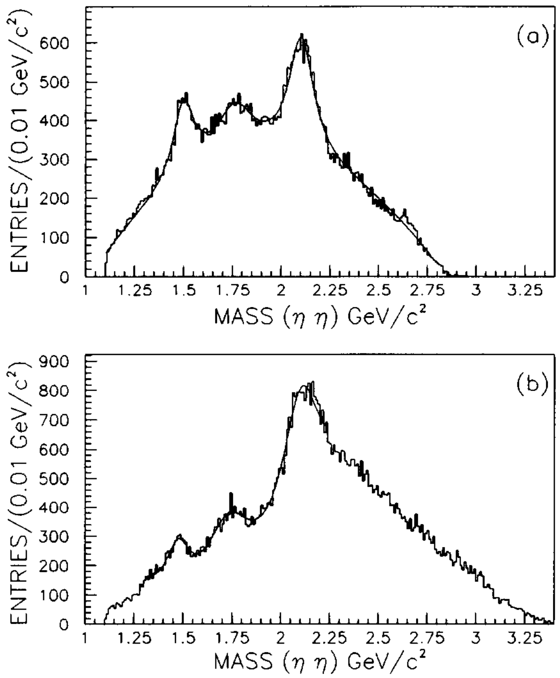

Fig. 3. $\eta\eta$ mass projections for reaction (3) at (a) 3.0 and (b) 3.5 GeV CM energy. The curves are fits to three states plus background. See text for details.

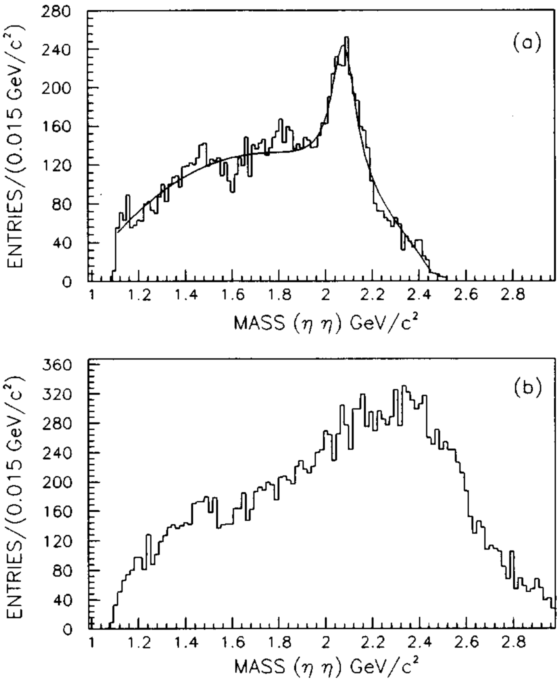

Fig. 4. $\eta\eta$ mass projections for reaction (4) at (a) 3.0 GeV and (b) 3.5 GeV CM energy. The curve is a fit to one state plus background. See text for details.

$$X(1500): \quad M = 1488 \pm 10\ \mathrm{MeV}/c^2,$$

$$\Gamma = 148 \pm 17\ \mathrm{MeV}/c^2,$$

$$X(1750): \quad M = 1748 \pm 10\ \mathrm{MeV}/c^2,$$

$$\Gamma = 264 \pm 25\ \mathrm{MeV}/c^2,$$

$$X(2100): \quad M = 2104 \pm 20\ \mathrm{MeV}/c^2,$$

$$\Gamma = 203 \pm 10\ \mathrm{MeV}/c^2.$$

The fit to fig. 3b has been restricted to $M < 2250$ MeV/c^2, since it is found that the region above this value cannot be described by a single additional Breit–Wigner plus background.

Fitting the $\eta\pi$ mass projection in the same way gives the following results for the mass and width of the $a_2(1320)$:

$$M = 1324 \pm 5\ \mathrm{MeV}/c^2, \quad \Gamma = 118 \pm 10\ \mathrm{MeV}/c^2.$$

These are in agreement with the accepted values for this resonance [4]. We have performed similar checks on other well-established states observed in our data, including $\omega(783)$, $\eta'(958)$ and $f_1(1285)$, which confirm (784±2, 958±3 and 1282±4 MeV respectively) the correctness of our mass scale.

For reaction (4), features which can be distinguished in the 3.0 GeV Dalitz plot are strong bands corresponding to a mass of approximately 2100 MeV/c^2, and an accumulation at the center of the plot where resonances in the range 1500–1900 MeV/c^2 would overlap. The Dalitz plot for the 3.5 GeV data suggests considerable structure in the 2000–2600 MeV/c^2 mass range. Figs. 4a, 4b show the $\eta\eta$ mass projections. For comparison with the $\pi\eta\eta$ results, we have attempted a fit to the 3.0 GeV data (fig. 4a) and find a mass and width of 2080 ± 20 and 131 ± 10 MeV/c^2 respectively for the 2100 MeV/c^2 state. At this time, we conjecture that the absence of a single isolated peak at 2100 MeV/c^2 in fig. 4b may be due to the existence of yet further $\eta\eta$ structure(s) at higher mass.

We now consider possible identification of these states with known resonances. In the case of the state we have labelled $X(1500)$, one possibility is that it is the $f_2(1520)$ recently observed in annihilations at rest by Aker et al. [5] with $M = 1515 \pm 10$ MeV/c^2, $\Gamma = 120 \pm 10$ MeV/c^2, and also in the present experiment [3]. If this is the same object, we estimate the ratio of its decays to 2η and $2\pi^0$ to be $2.4 \pm 0.5\%$, where the error is statistical only. Taking into account model-dependent assumptions for acceptance and background, we estimate that the systematic error on this ratio is of order 50%. This ratio is significantly larger than for the $f_2(1270)$, where it is 5.3×10^{-3} and the decay to $\eta\eta$ is limited by phase space. Another possibility is that we may be observing the $f_2'(1525)$, though at a mass lower than the accepted value. In fact, direct evidence for decay of the $f_2'(1525)$ to 2η is rather weak [6], and consistent with its being a lower-mass object in the $\eta\eta$ channel.

In the region of 1750 MeV/c^2, two possibilities present themselves: the narrow (< 80 MeV) $X(1740)$ seen by Alde et al. [7] and the well-established broad $f_0(1710)$, which has been observed [4] decaying to $\eta\eta$. Again, the evidence for the latter decay is weak. We see no evidence for the $f_0(1590)$ reported by Alde et al. [8].

The state at 2100 MeV/c^2 is also difficult to identify unambiguously. Of the known states in this region, the $f_4(2050)$ has a mass and width not much different from the values found above, but its reported branching ratio to $\eta\eta$ is too small to explain this large effect. The most likely candidate seems to be the $f_2(2175)$ seen by the GAMS Collaboration in central production [9]. Our observation of a $2\pi^0$ enhancement at a significantly lower mass of 1964 ± 35 MeV [3] provides little assistance in understanding this state.

We gratefully acknowledge technical support from our collaborating institutions and the outstanding contribution of the Fermilab Accelerator Division Antiproton Department. This work was funded by the US Department of Energy, the National Science Foundation, and the Italian Istituto Nazionale di Fisica Nucleare.

References

[1] T.A. Armstrong et al., Nucl. Phys. B 373 (1992) 35; Phys. Rev. Lett. 68 (1992) 1468.

[2] T.A. Armstrong et al., Measurement of the $\gamma\gamma$ partial width of the χ_2 resonance, submitted to Phys. Rev. Lett.

[3] T.A. Armstrong et al., Phys. Lett. B 307 (1993) 399.

[4] Particle Data Group, K. Hikasa et al., Review of particle properties, Phys. Rev. D 45 (1992) S1.

[5] E. Aker et al., Phys. Lett. B 260 (1991) 249.

[6] Y. Prokoshkin, 25th Intern. Conf. on High energy physics (Singapore, 1990) eds. K.K. Phua and Y. Yamaguchi (World Scientific, Singapore, 1991) p. 582.

[7] D. Alde et al., Phys. Lett. B 284 (1992) 457.

[8] D. Alde et al., Nucl. Phys. B 269 (1986) 485.

[9] Y. Prokoshkin, 3rd Intern. Conf. Hadron spectroscopy Hadron 89, (Ajaccio, France, September 1989) (Editions Frontières, Dreux) p. 27.